# Energy Level Alignment at the Anode of Poly(3-hexylthiophene)/Fullerene-Based Solar Cells

**Chih-Ping Chen,[†] Ta-Chang Tien,[*,†,‡] Bao-Tsan Ko,[†,§] Yeu-Ding Chen,[†] and Ching Ting[†]**

Material and Chemical Research Laboratories and Nanotechnology Research Center, Industrial Technology Research Institute, Hsinchu, Taiwan 310, Republic of China, and Department of Chemistry, Center for Nanotechnology, Chung-Yuan Christian University, Chung-Li, Taiwan 320, Republic of China

**ABSTRACT** We have used ultraviolet photoelectron spectroscopy to investigate the energy-level and band alignment near the anode for poly(3-hexylthiophene)/[6,6]-phenyl-$C_{61}$-butyric acid methyl ester (P3HT/PCBM)-based organic solar cells. Analysis of various batches of indium−tin oxide (ITO) revealed that the photoresist residues had a strong effect, reducing the work functions of ITO ($\Phi_{ITO}$) by as much as 0.61 eV. The energy-level alignment of poly(3,4-ethylenedioxythiophene)/ITO ($\Phi_{PEDOT/ITO}$) interfaces obey the Mott−Schottky rule at values of $\Phi_{ITO}$ of less than 3.92 eV. In contrast, we observed Fermi-level pinning for the blend/PEDOT interfaces at values of $\Phi_{PEDOT/ITO}$ greater than 4.26 eV; this finding is consistent with a previous report that the positive polaronic energy of P3HT is equal to 4.0 eV. Consequently, we suspect that the similar efficiency levels and open-circuit voltages of devices prepared from various ITO samples were due mainly to the constant interfacial energy barrier at the blend/PEDOT interface with Fermi-level pinning.

**KEYWORDS:** energy level • band alignment • P3HT−PCBM • organic solar cell

## INTRODUCTION

Nanocomposite organic solar cells (OSCs) are potential candidates for providing third-generation renewable energy, primarily because of their low manufacturing costs (1−3). The power conversion efficiency (PCE) of OSCs has been improved up to 5% under A.M.1.5G conditions (2, 4, 5) when incorporating a blend film of poly(3-hexylthiophene) (P3HT) as the donor and [6,6]-phenyl-$C_{61}$-butyric acid methyl ester (PCBM) as the acceptor. Most studies of P3HT/PCBM-based OSCs have focused on improving device processing and performance (1, 6); fewer experiments have been dedicated to determining the mechanism of carrier transport, particularly the transport effectiveness of carriers to the electrode contacts, or to analyzing the energy levels at the interface of the OSCs. At present, it is unclear how significant the role played by the interface of the OSCs is and how the efficiency may be improved further (7). For example, most energy diagrams of OSCs have been determined previously by comparing the ionization potential or electron affinity of the active layer components to the Fermi level of the contacts; indeed, the vacuum levels (VLs) of the two materials are typically assumed to be equal, which is rarely the case because the dipole at the interface or physicochemical interactions can shift the VL of the active components with respect to the Fermi level of the contacts (electrodes) at the interface (8). In this letter, we describe how ultraviolet photoelectron spectroscopy (UPS) (9) can be used to determine the carrier-transport properties at interfacial electronic structures so as to further understand the interfacial properties at the anodes of OSCs.

## EXPERIMENTAL SECTION

Three ITO films were chosen as transparent electrodes for the solar cells: X-ITO (Merck, 10 Ω/□), S-ITO (Sanyo, 8 Ω/□), and M-ITO (Merck, 5 Ω/□). All three films have transparency ratings of >80% for the transmission of visible light. The ITO films were sequentially patterned photolithographically, cleaned with a detergent, cleaned ultrasonically in a mixture of acetone and isopropyl alcohol, dried on a hot plate at 120 °C for 5 min, and exposed to oxygen plasma for 5 min. Poly(3,4-ethylenedioxythiophene)−poly(styrenesulfonate) (PEDOT−PSS, Baytron P-VP AI4083) was filtered through a 0.45-$\mu$m filter before being deposited on ITO at a thickness of ca. 30 nm through spin-coating at 3000 rpm in air. The electrodes were then dried at 150 °C for 30 min inside a glovebox. Using a solution of P3HT and PCBM (17 mg/mL; weight ratio = 1:0.9) in dichlorobenzene, thin films of the blend were placed on top of the PEDOT layer through spin-coating at 450−4000 rpm. The device was then annealed at 140 °C for 20 min in a glovebox; any remaining solvent was evaporated during this time. Finally, the device was subjected to thermal treatment until the evaporative process left a 30-nm-thick layer of Ca and a 100-nm-thick layer of Al. The samples of PEDOT and the blend films were moved into a desiccator in a glovebox under $N_2$ and then transferred to the UPS sample-loading chamber within 3 min. UPS spectra were recorded (VG ESCALab 250; HeI $h\nu$ = 21.22 eV) at a sample bias of −5 V to observe the secondary electron cutoff, from which the work function was derived.

## RESULTS AND DISCUSSION

Three compositional factors are known to affect the work function ($\Phi$) of ITO: the oxygen-to-indium (O/In) ratio, the

* To whom correspondence should be addressed. E-mail: tien@itri.org.tw.
Received for review December 22, 2008 and accepted March 16, 2009
† Material and Chemical Research Laboratories, Industrial Technology Research Institute.
‡ Nanotechnology Research Center, Industrial Technology Research Institute.
§ Chung-Yuan Christian University.
DOI: 10.1021/am800259h

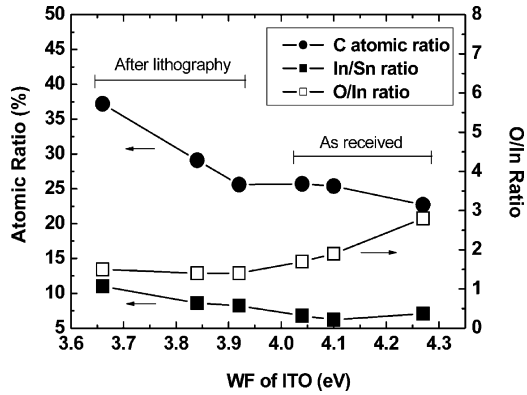


**FIGURE 1. Relationship between the work function and the chemical composition of ITO samples.**

carbon content, and the indium-to-tin (In/Sn) ratio. Inevitably, these factors affected the values of Φ of the ITO samples tested in this study because we subjected them to solution processing (10). We employed X-ray photoelectron spectroscopy (XPS) and UPS (Figure 1) to determine the effects of these compositions on the values of Φ of the three ITO samples. The work functions of the "as-received" and "after lithography" samples varied from 3.66 to 4.27 eV; they were inversely proportional to the carbon content and the In/Sn ratio but directly proportional to the O/In ratio. The value of Φ of the as-received S-ITO was 4.27 eV, which is in reasonable agreement with values determined using UPS for similarly prepared ITO samples (11, 12). After the ITO samples were subjected to lithographic processing, the carbon contents on the surfaces increased from 23 to 37.5%; the values of Φ decreased accordingly from 4.27 to 3.66 eV. Figure 1 reveals that the carbon concentration and the work function correlate quite well. It is possible that the decreasing value of Φ upon an increase in the extent of carbon contamination on the ITO surface was caused by the formation of an ionic double layer of opposite sign to the intrinsic dipole (13). On the other hand, a decrease in the Sn dopant concentration is expected to lower the Fermi level and increase the value of Φ (10). The O/In atomic ratio is affected by oxygen plasma treatment, which may be regarded as a process that adds oxygen vacancies onto ITO surfaces. Indeed, the oxygen content, as represented by the O/In atomic ratio, is proportional to the work function. In

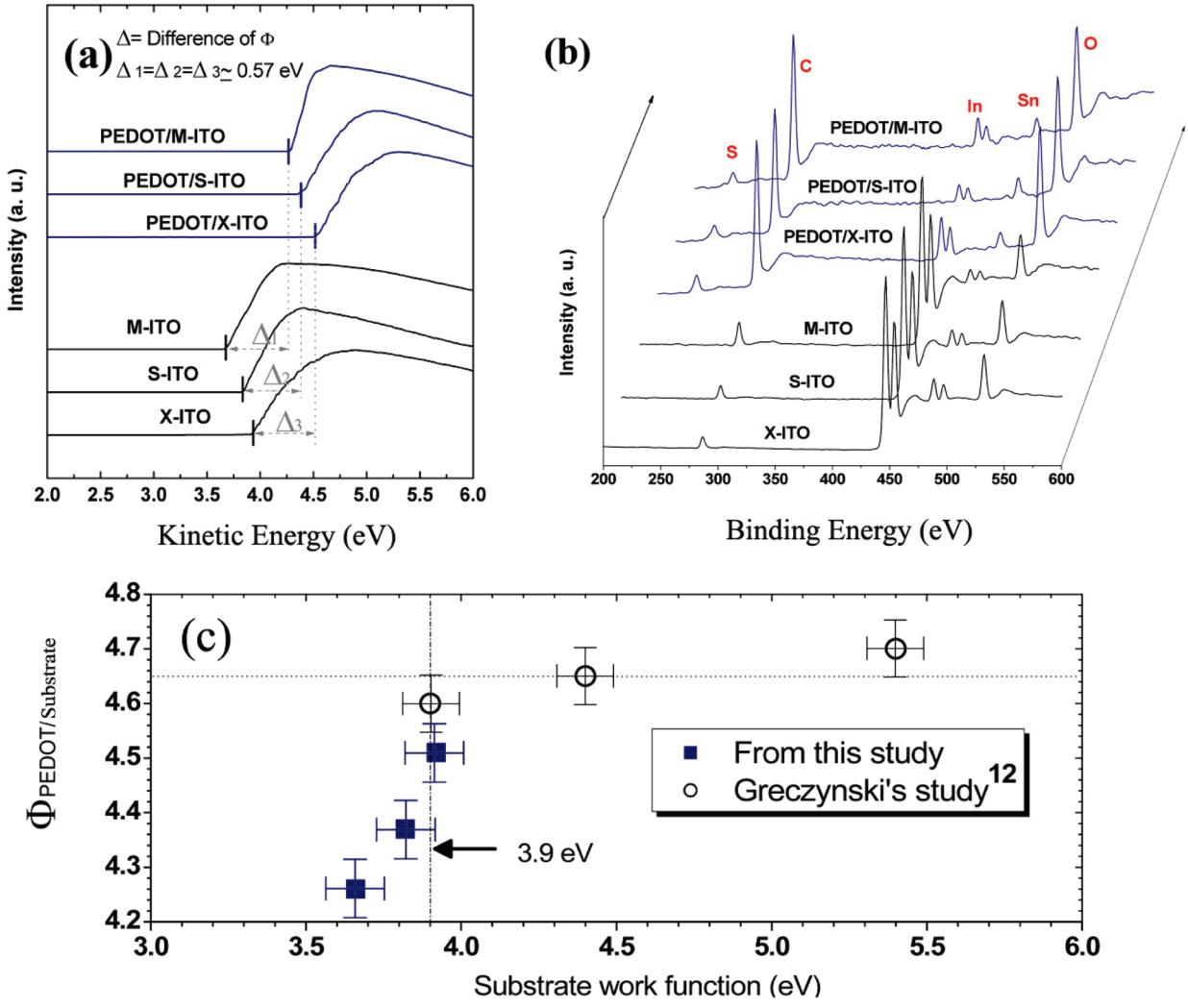


**FIGURE 2. (a) UPS of PEDOT/ITO interfaces and ITO films, (b) XPS of PEDOT/ITO interfaces and ITO films, and (c) dependence of the work function of PEDOT/ITO interfaces, $\Phi_{PEDOT/ITO}$, on the work function of substrates. Data points indicated by open symbols were adopted from ref (12).**

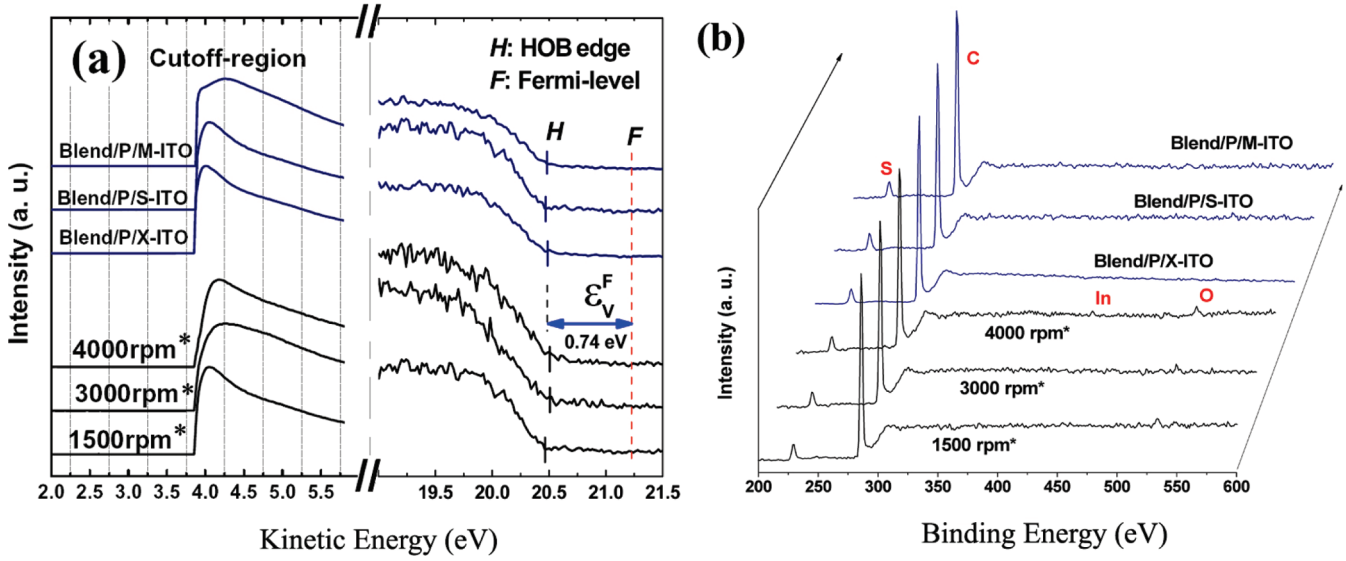


**FIGURE 3. Photoelectron spectra by (a) UPS of blend/PEDOT interfaces and (b) XPS of blend/PEDOT interfaces. *: The 1500, 3000, and 4000 rpm denote the spin-coating speeds of blend films on PEDOT/S-ITO, and the blend/P/various ITO were coated at 450 rpm (rpm = revolutions per minute).**

addition to the variations in the values of $\Phi$, our three ITO substrates exhibited several other distinct features. For example, the thicknesses of the ITO layers of X-ITO, S-ITO, and M-ITO were 210, 160, and 260 nm, respectively. Their transparencies were slightly different, following the order S-ITO > X-ITO > M-ITO. M-ITO had the highest conductivity, the thickest ITO layer, and the lowest transparency; its slightly higher conductivity meant that M-ITO had the advantageous property of providing the lowest sheet resistance when fabricating large-area solar cell modules. When using the ITO pattern procedure, however, its thicker ITO may cause problems during the etching process.

After application of a thin film of PEDOT, we recorded UPS and XPS spectra of the PEDOT/ITO samples [Figure 2a,b]. Because the detected depth was less than 10 nm based on both photoelectron spectra (14), the presence of In and Sn peaks at atomic ratios of greater than 5% in the XPS spectrum suggested that all of the signals in the UPS spectrum arose from the PEDOT/ITO interface (15). Not only were the values of $\Phi$ of the PEDOT/ITO samples proportional to the values of $\Phi$ of the original ITO surfaces, but the differences between the work functions ($\Delta_{PEDOT/ITO} = \Phi_{PEDOT/ITO} - \Phi_{ITO}$) were almost constant (ca. 0.57 eV) under a value of $\Phi_{ITO}$ of 3.92 eV. This interfacial phenomenon can be regarded as a type of VL alignment or as following the Mott–Schottky rule (16, 17); it occurs whenever the value of $\Phi$ of the substrate ($\Phi_{substrate}$) is smaller than the energy of the positive polaronic state of the organic compound. For example, if the value of $\Phi$ of the substrate is smaller than the positive polaronic energy of P3HT (ca. 4.0 eV) (18), the value of $\Phi$ of the P3HT/substrate is proportional to the value of $\Phi$ of the substrate. Interestingly, Greczynski et al. (19) reported that the work function of the PEDOT film is constant (Fermi-level pinning) for values of $\Phi_{substrate}$ in the range from 3.9 to 5.4 eV. In agreement with Greczynski's results, Figure 2c suggests that a value of 3.9 eV could be the boundary between VL alignment and Fermi-level pinning. Because we and Greczynski both used work functions measured from UPS spectra, the error in the work function depends on the "resolution" of UPS (ca. 0.1 eV). In Figure 2c, the error bars for our and Greczynski's data at 3.9 eV overlap one another, suggesting that the deviations between the two sets of data were within the range of spectral resolution. The fact that the values of $\Delta_{PEDOT/ITO}$ were the same and independent of the values of $\Phi$ of the ITO samples indicates that the formation of a dipole layer by a charged interface state occurred near the PEDOT/ITO interface (9). Therefore, we suspect that the same dipole might exist at the PEDOT/ITO interface, irrespective of the nature of the ITO substrate. A comprehensive understanding of this issue will require further studies that are beyond the scope of this paper.

Figure 3a presents the UPS results of the blend/PEDOT/S-ITO samples. The thicknesses of the blend films deposited at 1500, 3000, and 4000 rpm were 90, 40, and 30 nm, respectively. Figure 3b reveals the presence of In and O peaks in the XPS spectrum of the sample prepared at 4000 rpm, implying that these XPS/UPS signals originated from the blend/PEDOT interface. In the UPS spectra, we observed nearly the same energy level at each thickness. Table 1 indicates that the values of $\Phi$ of the blend films were close to 3.86 ± 0.01 eV and independent of the nature of the original PEDOT surface. A more detailed understanding of this relationship can be obtained from Figure 3a, which reveals that the highest occupied band edge of each blend film was nearly at the same energy level. The slope parameter ($S$) can be used to identify Fermi-level pinning of alignment regimes at organic/metal or organic/organic interfaces (18). In this case, the value of $S_{Blend/PEDOT}$ [determined using the expression $d(\Phi_{blend/PEDOT})/d(\Phi_{PEDOT/ITO})$] was zero (Table 1), thereby conserving the Fermi-level pinning of the alignment regime; i.e., there is an interfacial state possessing sufficient dipoles to pin the Fermi level of the semiconductor (20). It has been proposed that such a pinning phenomenon

Table 1. Experimental Energy Levels Measured by UPS

| substrate | $\Phi_{ITO}$ as-received | $\Phi_{ITO}$ after lithography | $\Phi_{PEDOT/ITO}$ | $\Phi_{blend/PEDOT}$ | $\Delta_{PEDOT/ITO}$ | $S_{blend/PEDOT}$ |
|---|---|---|---|---|---|---|
| X-ITO | 4.04 | 3.92 | 4.51 | 3.85 | 0.59 | ~0 |
| S-ITO | 4.27 | 3.82 | 4.37 | 3.87 | 0.55 | ~0 |
| M-ITO | 4.12 | 3.66 | 4.26 | 3.86 | 0.6 | ~0 |

[a] Unit: eV.

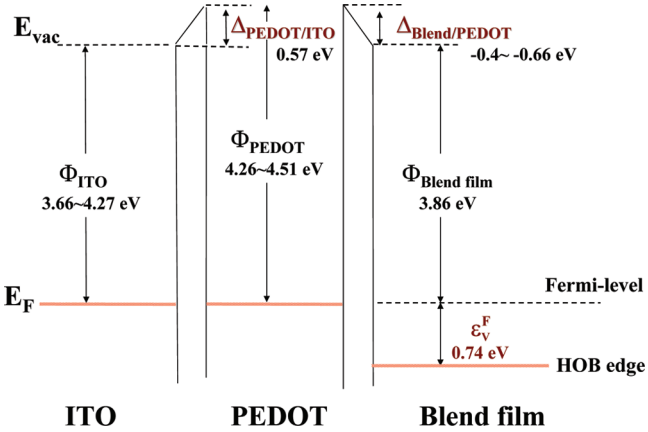


**FIGURE 4. Schematic band diagram representing the interfacial energy levels at the anode of a P3HT/PCBM solar cell obtained by UPS.**

may be caused by charge transfer between the conducting polymer and the organic semiconductor (21). As a result, the variation of the PEDOT work function did not affect the barrier height ($\varepsilon_V^F$) at the PEDOT/blend interface. A similar result was observed recently at the interface between copper phthalocyanine and PEDOT upon variation of the value of $\Phi$ (22).

On the basis of all of the results described above, Figure 4 presents a schematic representation of the band diagram of the anodes of the P3HT/PCBM-based solar cells prepared in this study. The obtained band diagram indicated that differences in the work functions ($\Delta$) of the PEDOT/ITO interface are the same values as the various substrate work functions (VL alignment or the Mott–Schottky rule) (16, 17); nevertheless, Fermi-level pinning controls the interfacial energy levels of the blend films (8, 18). For the first interface (PEDOT/ITO), although it is unclear why the various ITO samples provided a nearly constant value of $\Delta$, when hole transport occurred through the PEDOT/ITO interface, the built-in potential ($V_{bi}$) was constant and independent of the type of ITO (22) when the work function of ITO was less than 3.9 eV. In contrast, the differences in the work functions ($\Delta$) of the blend/PEDOT interfaces, reflected in the sizes of the dipoles, changed proportionally to the value of $\Phi$ of the ITO sample. The possibility of controlling the values of $\varepsilon_V^F$ via the properties of the individual substrates would be difficult if Fermi-level pinning occurs. From current–voltage ($I$–$V$) measurements obtained from a Peccell solar simulator using a programmable Keithley 2400 source at an intensity of 100 mW/cm$^2$, we found that the devices incorporating the various ITO substrates exhibited similar efficiencies. The devices exhibited PCEs of 3.9 ± 0.2 %, values of $J_{sc}$ of 9.9 ± 0.2 mA/cm$^2$, open-circuit voltages ($V_{oc}$) of 0.62 ± 0.02 V, and fill factors of 0.62 ± 0.02. The similar values of $V_{oc}$ arose primarily from the same interfacial charge barrier ($\varepsilon_V^F$) at the blend/PEDOT interfaces on the various ITO substrates. From a study of the relationship between the work function of PEDOT and the value of $V_{oc}$ in OSCs incorporating *p*-phenylenevinylene (PPV) and PEDOT layers, Frohne et al. proposed (23) that the change in the work function scaled exactly with the open-circuit voltage of the OSC, suggesting that no pinning occurred between the photoactive PPV and PEDOT layers. In our present study, we suggest that the existence of Fermi-level pinning between the photoactive and PEDOT layers depended on the work function of ITO and the positive polaronic energy of the photoactive layer.

## SUMMARY

Using UPS, we developed a band diagram for the relationship between the anodes and active layers of solar cell devices that describes the effects of changes to the work function of the ITO sample. We found that the work functions of PEDOT/ITO interfaces obey the Mott–Schottky rule at values of $\Phi_{ITO}$ of less than 3.92 eV. In contrast, the energy levels of the blend/PEDOT interfaces prepared in this study exhibited Fermi-level pinning at values of $\Phi_{PEDOT/ITO}$ of greater than 4.26 eV. The same value of the interfacial charge barrier ($\varepsilon_V^F$) induced by Fermi-level pinning at the various blend/PEDOT interfaces may explain the similar OSC performances of all of our tested devices.

## REFERENCES AND NOTES


(1) Gunes, S.; Neugebauer, H.; Sariciftci, N. S. *Chem. Rev.* **2007**, *107*, 1324.
(2) Kim, J. Y.; Lee, K.; Coates, N. E.; Moses, D.; Nguyen, T. Q.; Dante, M.; Heeger, A. J. *Science* **2007**, *317*, 222.
(3) Gur, I.; Fromer, N.; Chen, C. P.; Kanarkas, A.; Alivisatos, A. P. *Nano Lett.* **2007**, *7*, 409.
(4) Kim, J. Y.; Kim, S. H.; Lee, H.; Lee, H. K.; Ma, W.; Gong, X.; Heeger, A. J. *Adv. Mater.* **2006**, *18*, 572.
(5) Li, G.; Shrotriya, V.; Huang, J.; Yao, Y.; Mariarty, T.; Emery, K.; Yang, Y. *Nat. Mater.* **2005**, *4*, 864.
(6) Scharber, M. C.; Muhlbacher, D.; Koppe, M.; Denk, P.; Waldauf, C.; Heeger, A. J.; Brabec, C. *Adv. Mater.* **2006**, *18*, 789.
(7) Koster, L. J.; Mihailetchi, V. D.; Blom, P. W. *Appl. Phys. Lett.* **2006**, *88*, 093511.
(8) Murdey, R. J.; Salaneck, W. R. *Jpn. J. Appl. Phys.* **2005**, *44*, 3751.
(9) Ishii, H.; Sugiyama, K.; Ito, E.; Seki, K. *Adv. Mater.* **1999**, *8*, 605.
(10) Sugiyama, K.; Ishii, H.; Ouchi, Y.; Seki, K. *J. Appl. Phys.* **2000**, *87*, 295.
(11) Fukagawa, H.; Kera, S.; Kataoka, T.; Hosoumi, S.; Watanabe, Y.; Kudo, K.; Ueno, N. *Adv. Mater.* **2007**, *19*, 665.
(12) Schlaf, R.; Murata, H.; Kafafi, Z. H. *J. Electron Spectrosc. Relat. Phenom.* **2001**, *120*, 149.
(13) Ishii, M.; Mori, T.; Fujikawa, H.; Tokito, S.; Taga, Y. *J. Lumin.* **2000**, *87*, 1165.

(14) Briggs, D.; Seah, M. P. *Practical Surface Analysis: By Auger and X-Ray Photoelectron Spectroscopy* ; John Wiley & Sons: New York, 1983; p 33.
(15) Jong, M. P.; IJzendoorn, L. J.; Voigt, M. J. A. *Appl. Phys. Lett.* **2000**, *77*, 2255.
(16) Davids, P. S.; Saxena, A.; Smith, D. L. *J. Appl. Phys.* **1995**, *78*, 4244.
(17) Davids, P. S.; Saxena, A.; Smith, D. L. *Phys. Rev. B* **1996**, *53*, 4823.
(18) Tengstedt, C.; Osikowicz, W.; Salaneck, W. R.; Parker, I. D.; Hsu, C. H.; Fahlman, M. *Appl. Phys. Lett.* **2006**, *88*, 0353502.
(19) Greczynski, G.; Kugler, Th.; Keil, M.; Osikowicz, W.; Fahlman, M.; Salaneck, W. R. *J. Electron Spectrosc. Relat. Phenom.* **2001**, *120*, 149.
(20) Ito, E.; Oji, H.; Ishii, H.; Oichi, K.; Ouchi, Y.; Seki, K. *Chem. Phys. Lett.* **1999**, *287*, 137.
(21) Peisert, H.; Knupfer, M.; Zhang, F.; Petr, A.; Dunsch, L.; Fink, J. *Appl. Phys. Lett.* **2003**, *83*, 3930.
(22) Peisert, H.; Petr, A.; Dunsch, L.; Chass, T.; Knupfer, M. *ChemPhysChem* **2007**, *8*, 386.
(23) Frohne, H.; Shaheen, S. E.; Brabec, C. J.; Muller, D. C.; Sariciftci, N. S.; Meerholz, K. *ChemPhysChem* **2002**, *3*, 795.

AM800259H